IOP Publishing | Institute of Physics and Engineering in Medicine Physics in Medicine & Biology

Phys. Med. Biol. **61** (2016) 1596–1607 doi:10.1088/0031-9155/61/4/1596

In vivo electric conductivity of cervical cancer patients based on B_1^+ maps at 3T MRI

E Balidemaj[1], P de Boer[1], A L H M W van Lier[2], R F Remis[3], L J A Stalpers[1], G H Westerveld[1], A J Nederveen[3], C A T van den Berg[2] and J Crezee[1]

[1] Radiotherapy, Academic Medical Center, Amsterdam, The Netherlands
[2] Radiotherapy, University Medical Center Utrecht, Utrecht, The Netherlands
[3] Circuits and Systems Group, Delft University of Technology, Delft, The Netherlands
[4] Radiology, Academic Medical Center, Amsterdam, The Netherlands

E-mail: edmondbalidemaj@gmail.com

Received 14 September 2015, revised 21 December 2015
Accepted for publication 5 January 2016
Published 2 February 2016

Abstract

The *in vivo* electric conductivity (σ) values of tissue are essential for accurate electromagnetic simulations and specific absorption rate (SAR) assessment for applications such as thermal dose computations in hyperthermia. Currently used σ-values are mostly based on *ex vivo* measurements. In this study the conductivity of human muscle, bladder content and cervical tumors is acquired non-invasively *in vivo* using MRI.

The conductivity of 20 cervical cancer patients was measured with the MR-based electric properties tomography method on a standard 3T MRI system.

The average *in vivo* σ-value of muscle is 14% higher than currently used in human simulation models. The σ-value of bladder content is an order of magnitude higher than the value for bladder wall tissue that is used for the complete bladder in many models. Our findings are confirmed by various *in vivo* animal studies from the literature. In cervical tumors, the observed average conductivity was 13% higher than the literature value reported for cervical tissue.

Considerable deviations were found for the electrical conductivity observed in this study and the commonly used values for SAR assessment, emphasizing the importance of acquiring *in vivo* conductivity for more accurate SAR assessment in various applications.

Keywords: EPT, conductivity, electrical conductivity, dielectric properties, hyperthermia

(Some figures may appear in colour only in the online journal)

Introduction

Accurate tissue electric properties (conductivity and permittivity) are critical for correct electromagnetic simulations and subsequent specific absorption rate (SAR) assessment for various purposes, such as for the safety assessment of magnetic resonance imaging (MRI) (Katscher *et al* 2009, Zhang *et al* 2013) and telecommunications (Peyman *et al* 2009) or for thermal dose computation in hyperthermia treatment planning (HTP) (de Greef *et al* 2011). SAR is related to conductivity (σ) as $\mathrm{SAR} = \sigma |E|^2/(2\rho)$, where E is the electric field and ρ is the tissue density. Since many of the electric properties used in human models are based on *ex vivo* measurements of animal and human tissues (Gabriel 1996, Gabriel *et al* 1996b), the accuracy of *in vivo* SAR determination in specific applications may be questionable. Furthermore, a review of those measurements from many studies showed a large variation between the reported electrical properties (Gabriel *et al* 1996a). These variations can be explained by the use of tissues of various species and variations in measuring conditions (tissue temperature, *in vivo*, *in vitro* and *ex vivo*). Based on this disparity, we believe that there is sufficient reason to verify the validity of the currently maintained *in vivo* electric property values.

Due to practical and ethical reasons, human *in vivo* electric property measurements are scarce. Only easily accessible tissue types (e.g. skin, tongue) (Gabriel *et al* 1996b) and the liver (O'Rourke *et al* 2007) have been measured *in vivo*. Therefore, MR-based methods to measure electric properties non-invasively have recently received increased attention. Electric properties tomography (EPT) (Katscher *et al* 2009, van Lier *et al* 2013, Balidemaj *et al* 2014, Liu *et al* 2015) is one such non-invasive technique to reconstruct electric properties using B_1^+ field measurements acquired by standard MR techniques. EPT has been previously applied for the *in vivo* electric property reconstruction of human brain tissue (Voigt *et al* 2011a, Van Lier *et al* 2013, Liu *et al* 2015) and the liver (Stehning *et al* 2012, Kim *et al* 2013). In these studies good agreement was shown between the mean reconstructed values and probe measurements reported in the literature, and typically a standard deviation of around 20% is observed. As in general the conductivity values of tumors are elevated compared to healthy tissue, EPT is a potential tool for tumor characterization and has recently been utilized to reconstruct the conductivity values of gliomas (Van Lier *et al* 2011, Voigt *et al* 2011b) and breast tumors (Katscher *et al* 2013, Shin *et al* 2014). One of the limitations of EPT is the accuracy at tissue boundaries due to kernel-based implementations and the use of the transceive phase assumption; therefore, various studies have investigated these issues (Sodickson *et al* 2013, Hafalir *et al* 2014, Balidemaj *et al* 2015a, Liu *et al* 2015).

In this work we utilize this technique to reconstruct the *in vivo* electric conductivity of tissues in the pelvic region. These results can be used for more accurate SAR determination in the HTP of deeply seated pelvic tumors. Here, we report the conductivity of muscle, bladder and cervical tumor as reconstructed using EPT, based on measurements performed at 3T MRI. Finally, we compare those values to the conductivity values reported in the literature for those tissue types.

Methods

In vivo MR measurements were conducted on 20 patients with cervical cancer in accordance with the approval of the Medical Ethics Board. 18 patients were histopathologically diagnosed with squamous-cell carcinoma (SCC) of the cervix; one was diagnosed with adenocarcinoma and one with endometrial carcinoma. Peristaltic bowel motion during the MRI scan was reduced with the intravenous injection of *Buscopan*® (Boehringer Ingelheim GmbH).

MR measurements

All experiments were conducted on a 3T MR system (Ingenia, Philips Healthcare, The Netherlands) using a 26-channel torso receive array. The B_1^+ amplitude map was acquired using the actual flip angle imaging (AFI) method (Yarnykh 2007) (3D, nom. flip angle = 65°, TR1/TR2 = 50/290 ms, 2.5 × 2.5 × 5mm, 16 slices, scan duration ≈ 6 min). The transceive phase was acquired by a spin echo (SE) sequence (repetition time (TR) = 1200 ms, 2.5 × 2.5 × 5 mm, 16 slices, scan duration ≈ 6 min) (Voigt *et al* 2011a, van Lier *et al* 2012b). Receiver non-uniformity including the phase contribution of the receive array was eliminated by using the so-called CLEAR technique (Voigt *et al* 2012). The net effect of this technique is that the phase of the receive array is replaced by the receive phase contribution of the system's birdcage body coil operated in reverse quadrature. To correct for eddy currents, the transceive phase was measured twice with opposing gradients (van Lier *et al* 2012a). Due to scan time limitations, a 5 mm isotropic resolution was used for 13 patients.

EPT reconstruction

The EPT reconstructions were performed using B_1^+ amplitude measurements and transceive phase approximation ($\phi^+ \approx \phi^{\pm}/2$) was applied as described in literature (Katscher *et al* 2009, Voigt *et al* 2011a, van Lier *et al* 2012a, 2013).

Assuming that the dielectric properties are piece-wise constant, the tissue electric conductivity can be computed by the homogeneous Helmholtz equation:

$$\frac{\nabla^2 B_1^+}{B_1^+} = -\mu_0 \varepsilon_0 \varepsilon_r \omega^2 - \mathrm{i}\mu_0 \sigma \omega, \tag{1}$$

where B_1^+ is the complex transmit field ($B_1^+ = \left|B_1^+\right| \mathrm{e}^{\mathrm{i}\phi^+}$), ε_r and σ are the relative permittivity and conductivity of the object of interest, respectively, ω is the Larmor angular frequency, and μ_0 and ε_0 are the permeability and permittivity of vacuum, respectively.

The conductivity can be computed by

$$\sigma = -\mathrm{Im}\left(\frac{\nabla^2\left(\left|B_1^+\right| \mathrm{e}^{\mathrm{i}\phi^+}\right)}{\left|B_1^+\right| \mathrm{e}^{\mathrm{i}\phi^+}}\right)\frac{1}{\mu_0\omega} = \frac{1}{\mu_0\omega}\left(\nabla^2\phi^+ + 2\frac{\nabla\left|B_1^+\right| \cdot \nabla\phi^+}{\left|B_1^+\right|}\right) \tag{2}$$

where in the last part of equation (2), the identity $\nabla \mathrm{e}^{\mathrm{i}\phi^+} = \mathrm{e}^{\mathrm{i}\phi^+}\mathrm{i}\nabla\phi^+$ was used (van Lier 2012).

The Laplacian required to evaluate equation (2) was computed by a kernel-based method as described in (van Lier *et al* 2012a) using a kernel size of 7 × 7 × 5 voxels. This noise-robust kernel was used to reduce the effect of noise on the second derivative. The applied EPT method in this study was validated in a pelvic-sized phantom study in Balidemaj *et al* (2014) where good agreement was found between EPT-based conductivity values and probe measurements (Model 85070C, HP/Agilent Corp, Santa Clara CA).

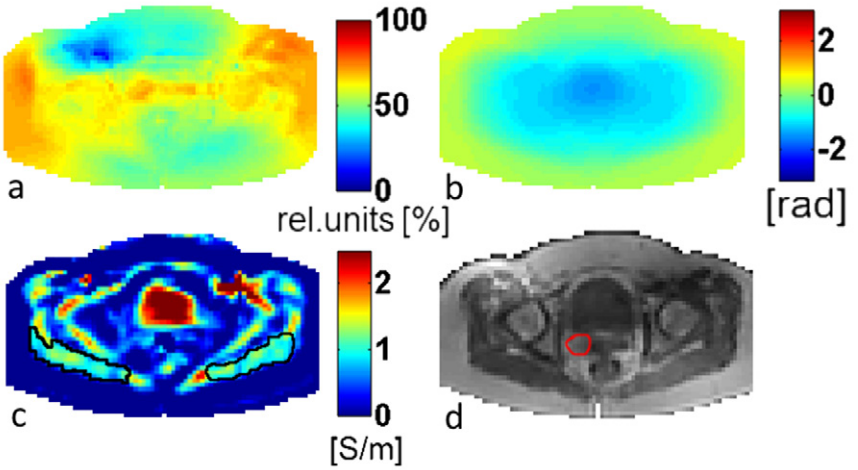

Figure 1. B_1^+ amplitude (a) and the transceive phase (b) of a patient. The reconstructed conductivity map (c) based on (a,b) and the corresponding T1 weighted image (d) acquired during the AFI sequence. The muscle delineation shown in black (c) excludes the EPT related boundary artifacts. The outline of the tumor is shown in red (d).

Quantification in vivo data

Tumor volume was delineated by a radiation oncologist based on CT and T2-weighted MRI images (TR/TE = 5906/80 ms, $0.70 \times 0.90 \times 3.00$ mm). *In vivo* MR measurements were used to reconstruct the electric conductivity and the reconstructed values were compared to literature values.

The average conductivity values were computed for all voxels inside a (manually) delineated volume-of-interest. All acquired slices have been used for the computations of the average and standard deviation of the σ-values. To exclude the effect of boundary reconstruction errors related to EPT, the delineated regions excluded boundaries where out-of-range σ-values were reconstructed. Furthermore, the first two pixels closest to the boundary were excluded and for a reliable reconstruction only tissues with a volume of at least $3.5 \times 3.5 \times 3.0$ cm^3 were considered. At the boundaries the reconstructed values can be twice as high as the expected values and are therefore excluded by excluding the first two pixels closest to the boundary. As a consequence the bladder and tumor volumes of only ten patients were sufficiently large to be included. All patients met the inclusion criteria for muscle tissue reconstructions. Computations regarding EPT reconstruction were performed using MATLAB® (The Mathworks, Natick, MA, U.S.).

Results

In figures 1(a) and (b), an example is depicted of the measured B_1^+ amplitude and transceive phase maps of a patient, respectively. The reconstructed σ-map based on figures 1(a) and (b) is shown in figure 1(c). Figure 1(c) also shows the manual delineation of muscle tissue to exclude EPT-related boundary artifacts from the measurement. The T1-weighted image of the patient, acquired by the AFI sequence, is shown for anatomical reference in figure 1(d).

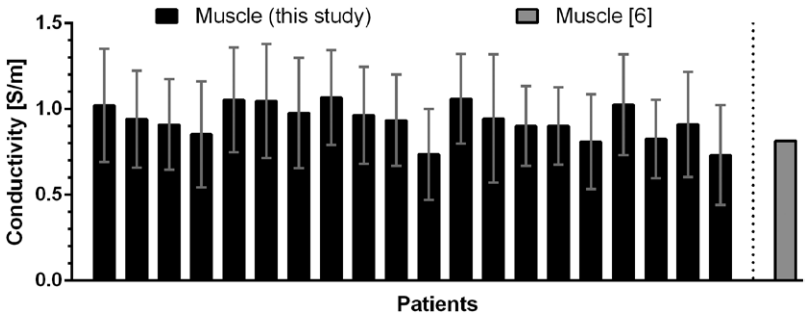

Figure 2. Muscle conductivity (mean ± std) of each patient and the literature value based on Gabriel (1996) at 128 MHz.

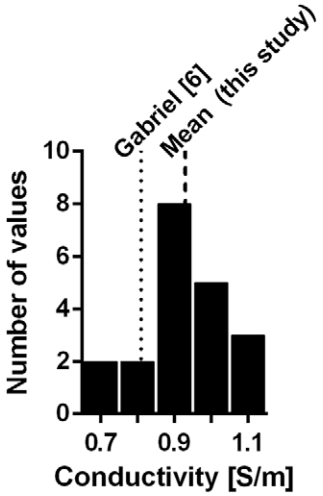

Figure 3. Distribution of the muscle data of 20 patients.

Muscle

In figure 2 the electric conductivity (mean ± std) of the muscle of each patient is presented. The mean conductivity value of muscle found in this study is 0.93 ± 0.26 S m^{-1}. In figure 2 the literature value as given by Gabriel (1996) is also shown, a value widely used in human models for SAR assessment in various applications. The mean value found in this study is 14% higher than the value reported in Gabriel (1996). In figure 3 the distribution of the data of the 20 patients is presented along with the mean value and the value based on Gabriel (1996).

Bladder content/urine

The reconstructed electric σ-values of the bladder content of ten patients are presented in figure 4. The interpatient variation is larger compared to the muscle conductivity. The mean value based on this study is 1.76 ± 0.42 S m^{-1}. The conductivity of urinary bladder wall tissue from the literature (Gabriel *et al* 1996b, Andreuccetti *et al* 1997) is also shown, which is widely used for the whole bladder volume in human models (Amjad 2007, Saunders and Aragon Zavala 2007, Fenn 2008, Homann 2012). Finally, the porcine urine conductivity value at 128 MHz, based on Peyman and Gabriel (2012), is also depicted in figure 4.

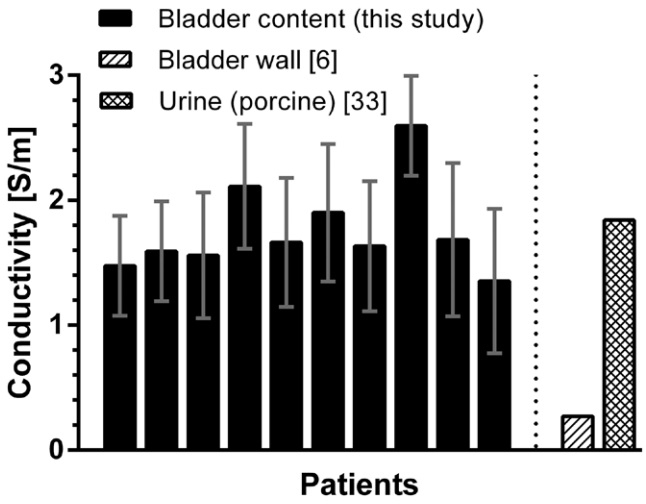

Figure 4. Bladder content conductivity based on this study and the literature value (Gabriel 1996) based on bladder wall tissue. The last bar represents the conductivity value of porcine urine reported in Peyman and Gabriel (2012).

Cervical tumor

In figure 5 the reconstructed electric σ-values of tumor tissues are depicted. The σ-value of adenocarcinoma and endometrial carcinoma is slightly higher than for other tumor tissues. The conductivity of cervical tissue at 128 MHz as reported in Gabriel (1996) is also shown in figure 5. The mean value of all cervical tumors is 1.02 ± 0.29 S m^{-1} which is 13% higher than the σ-value reported in Gabriel (1996).

Discussion

We have presented *in vivo* electrical σ-values as reconstructed by the EPT method based on B_1^+ data. The presented values correspond to σ-values at 128 MHz as this is the Larmor frequency of a 3T MR system.

Since current implementations of EPT might show error artifacts at tissue boundaries, these regions have been excluded from the calculation of the mean conductivity. However, the performance of the EPT of relatively large tissue regions is reliable as was demonstrated in the pelvic-sized phantom experiments in Balidemaj *et al* (2014) and brain studies (Voigt *et al* 2011a, van Lier *et al* 2013, Liu *et al* 2015). Furthermore, we applied transceive phase approximation, which was shown to hold for the pelvis anatomy in Balidemaj *et al* (2014). The standard deviation observed in this study and generally observed in EPT *in vivo* studies is due to the numerical implementation of the method and the heterogeneity of biological tissue. For instance, derivative operators act on typically noisy B1 data which together with the transceive phase approximation introduce around 20% standard deviation within a sample volume. Various studies have focused on the clinical implementation of new approaches increasing accuracy by using multi-transmit-channel systems or avoiding derivative operators (Liu *et al* 2013, Marques *et al* 2015, Balidemaj *et al* 2015a, Liu *et al* 2015). However, the close agreement between the reconstructed values of the 20 patients included in this study demonstrates the high reproducibility of the reconstructed conductivity values. Furthermore, we had repeat measurements available for three patients as they underwent a follow-up MR

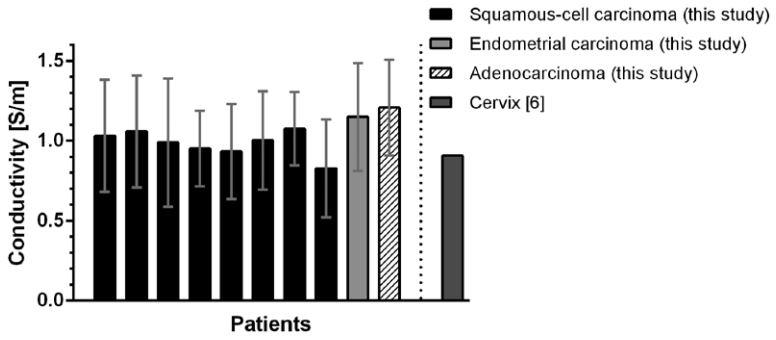

Figure 5. Cervical tumor σ-values observed in this study for squamous-cell carcinoma, adenocarcinoma and endometrial carcinoma compared to literature value.

scan after the treatment. The mean reconstructed muscle conductivity values in these three cases deviated less than 5% from the initially reconstructed conductivity values confirming the high reproducibility.

In general EPT is able to reconstruct permittivity values as well. However, the reconstruction accuracy varies with the field strength as shown earlier by van Lier *et al* (2013). It was shown that permittivity reconstruction *in vivo* is most accurate at 7T. Due to the limited accuracy of permittivity reconstruction at 3T we have focused on conductivity reconstruction only, since the acquisition of the latter contributes more substantially to more accurate SAR assessment. This was shown by Restivo *et al* (2016) for tumor SAR assessment at 7T MRI and in deep hyperthermia studies in Van De Kamer *et al* (2001), de Greef *et al* (2011), Canters *et al* (2013) and Balidemaj *et al* (2015b).

Currently, most of the electric property values presented in overviews like Gabriel *et al* (1996a) are measured under different measurement conditions; hence a large variance in values is reported. We have compared the σ-values reported in this study to the ones reported in the literature for the relevant frequency range, and included literature data available from animal studies at around body temperatures and human data at any temperature measured *in vivo*, *in vitro* or *ex vivo*.

Literature data are mostly presented in tables at distinct frequencies or in graphs. The latter necessitate the estimation of σ-values at intermediate frequencies by interpolation. We have chosen to consider only studies which presented data for muscle tissue at 100 MHz. In addition, we have included literature data at 128 MHz (i.e. Larmor frequency for 3T proton MRI) if this was explicitly given or if Cole–Cole parameters were reported allowing computation of the value at 128MHz. In general, the frequency dependence of tissue conductivity can be described by a Cole–Cole equation (Cole and Cole 1941).

Muscle

The comparison of our measured values to the values in the literature is challenging as conductivity measurements of human muscle are reported in just two studies (Schwan 1955, Joines *et al* 1994). In Joines *et al* (1994), measurements were performed between 1 and 2 h after excision at a temperature between 23 and 25 °C. No information regarding measuring conditions is provided in Schwan (1955). Note that the currently used conductivity value for muscle, based on Gabriel (1996), is of ovine origin, measured *ex vivo* (at 37 °C), and within 2 h after the animal is sacrificed. A larger overview of literature data for the muscle tissue of

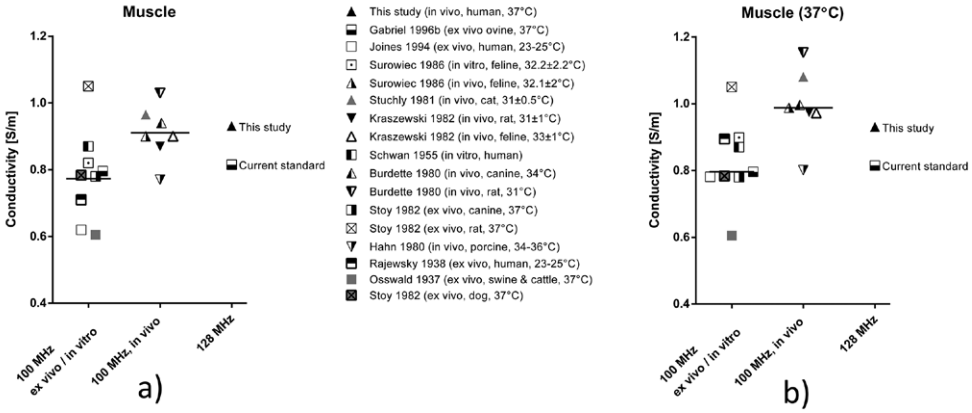

Figure 6. (a) An overview of the available literature data at 100 MHz and 128 MHz for the conductivity of muscle along with the mean value based on this study. (b) The literature data extrapolated to 37 °C by adjusting the conductivity values by 2%/°C. The horizontal line represents the median values of the *ex vivo*/*in vitro* data or the *in vivo* data.

different species and obtained both *in vivo* and *ex vivo* is depicted in figure 6(a). In figure 6(a) we have depicted the median of the reported σ-values in Osswald (1937), Stuchly *et al* (1981) and Stoy *et al* (1982). All the other values shown in figure 6(a) are mean values as reported in the corresponding studies (Rajewski 1938, Burdette *et al* 1980, Hahn *et al* 1980, Kraszewski *et al* 1982, Surowiect *et al* 1986). In figure 6(b) the temperature dependency of conductivity values is taken into account; therefore, the values of figure 6(a) are extrapolated to 37 °C by adjusting the values with 2%/°C as reported in Stogryn (1971) and Leussler *et al* (2012). The mean value found in this study is depicted alongside the literature values and appears to be in good agreement with the *in vivo* values reported in the literature for different species.

Thus, based on the σ-values reconstructed in this work, it is observed that the mean conductivity value of all the patients is approximately 14% higher than the value reported in Gabriel (1996). These findings are in agreement with animal studies presenting *in vivo* σ-values as shown in figure 6. We therefore reason that the currently used value for muscle conductivity slightly underestimates the true *in vivo* conductivity value; however, the reported value in Gabriel (1996) falls within the uncertainty range of the data presented in this study. The explanation for this 14% difference might be the higher blood and water content in living conditions. In Burdette *et al* (1986) and Schmid *et al* (2003) the effect on conductivity change after sacrifice was investigated for canine and porcine brain tissue, respectively, and a 15% conductivity decrease in the first 15 min after sacrifice was observed. Additionally, the physiological difference between human and ovine muscle tissue may explain the difference between the literature values and the values observed in this study. We have, furthermore, noticed that the conductivity value reported for muscle in the table in Gabriel (1996) is around 14% higher than reported in the online databases (Andreuccetti *et al* 1997, Hasgall *et al* 2015). We assume this discrepancy is introduced due to the use of Cole–Cole parameters in the latter databases which might lead to a mismatch at some frequencies compared to the true measurements (Gabriel 1996) which these Cole–Cole parameters are derived from.

Furthermore, Peyman *et al* (2001) reported a decrease of conductivity with age for various rat tissues, including muscle, in a frequency range of 130 MHz to 10 GHz, attributed to changes in cell sizes, structure, water content and the ratio of free to bound water. Based on

the Cole–Cole parameters presented in Peyman *et al* (2001, 2002), the estimated σ-values at 130 MHz of a newborn and 70 d-old rat muscle are 1.46 S m^{-1} and 0.68 S m^{-1}, respectively. In our study patient age ranged between 30 and 86 years; however, no significant age-related conductivity differences were observed in the relatively small patient population included in the study.

Bladder content/urine

There is a large discrepancy of an order of magnitude between the often used conductivity for bladder volume in human models (Amjad 2007, Saunders and Aragon Zavala 2007, Fenn 2008, Homann 2012) and the *in vivo* reconstructed conductivity based on EPT (figure 4). No study reports human urine σ-values at 128 MHz, but one study (Peyman and Gabriel 2012) reports σ-values of porcine urine using samples of 21 animals (at 37 °C). These yield, based on the reported Cole–Cole fitting parameters, a conductivity value of urine of 1.84 S m^{-1} at 128 MHz, which is in good agreement with the human values found in this study (figure 5). The reported root-mean-square-error of the fit was large (Peyman and Gabriel 2012), indicating a relatively large spread among the samples. The results of the porcine study (Peyman and Gabriel 2012) were recently included in the online database (Hasgall *et al* 2015); however, various SAR studies have been using the low conductivity value of bladder wall tissue for the whole bladder. There is one study reporting that human urine conductivity at 90 MHz is 1.81 (S m^{-1}) (Yuan *et al* 2012) measured by an impedance probe (Model 85070C, HP/Agilent Corp, Santa Clara CA) which is in good agreement with our findings.

Cervical tumor

The only available data on human cervical tissue at 128 MHz are found in Gabriel (1996) which are based on measurements (at 37 °C) on excised non-specified (healthy or tumor) cervical tissue. The reported σ-value is 0.91 S m^{-1}. In contrast, the cervix conductivity value used in, for instance, virtual family models (Hasgall *et al* 2015) and in the online available database (Andreuccetti *et al* 1997) is much lower: 0.75 S m^{-1} (at 128 MHz). The σ-value at 128 MHz based on Gabriel (1996) is shown in figure 5.

To the best of our knowledge, no data are available regarding cervical tumor σ-values at 128 MHz. The only reports on cervical tumor conductivity are based on measurements at 4.8 kHz and 614 kHz (Trokhanova *et al* 2010), where no significant difference in average σ-values has been observed between healthy and pathological cervix uteri. However, Trokhanova *et al* (2010) did observe a higher electrical conductivity value within the zone of the external fauces.

The average conductivity found in cervical tumors in this study is approximately 13% higher compared to Gabriel (1996). In our study however, we have not reconstructed the conductivity of healthy cervical tissue for comparison. We therefore have insufficient evidence to expect that our EPT technique is capable of differentiating this particular tumor type. We do not exclude of course that this technique is capable of differentiating other types of pelvic tumors provided the tumor is large enough and provided that this tumor type has conductivity properties which deviate more significantly from the surrounding normal tissue as was the case for the breast tumors evaluated by Katscher *et al* (2013). A further comparison between healthy and diseased cervical tissue is warranted to enable interpretation of the observed differences.

Conclusion

This study indicates that human *in vivo* electric conductivity values appear to deviate slightly from the values provided in the present databases at the investigated frequency and conductivity values should therefore be evaluated in a larger *in vivo* study investigating more human tissues. The *in vivo* values reported in this study were in good agreement with available *in vivo* data from the literature. The presented results have an impact on power absorption computations, used among others for HTP, emphasizing the importance of using *in vivo* values when incorporating electric conductivity data into numerical models.

Acknowledgments

This study was supported by grant UVA 2010–4660 of the Dutch Cancer Society.

References

Amjad A 2007 Specific absorption rate during magnetic resonance imaging *PhD Dissertation*

Andreuccetti D, Fossi R and Petrucci C 1997 An internet resource for the calculation of the dielectric properties of body tissues in the frequency range 10 Hz–100 GHz *IFAC-CNR* (*Florence, Italy*) (http://niremf.ifac.cnr.it/tissprop/)

Balidemaj E *et al* 2015a CSI-EPT: a contrast source inversion approach for improved MRI-based electric properties tomography *IEEE Trans. Med. Imaging* **34** 1788–96

Balidemaj E *et al* 2015b Hyperthermia treatment planning for cervical cancer patients based on electric conductivity tissue properties acquired *in vivo* from B1 + maps with EPT at 3T MRI *Int. J. Hyperth.* at press

Balidemaj E, Van Lier A L H M W, Crezee H, Nederveen A J, Stalpers L J A and Van Den Berg C A T 2014 Feasibility of electric property tomography of pelvic tumors at 3 T *Magn. Reson. Med.* **73** 1505–13

Burdette E C, Cain F L and Seals J 1980 *In vivo* probe measurement technique for determining dielectric properties at VHF through microwave frequencies *IEEE Trans. Microw. Theory Tech.* **MTT-28** 414–27

Burdette E C, Friederich P G, Seaman R L and Larsen L E 1986 *In situ* permittivity of canine brain: regional variations and postmortem changes *IEEE Trans. Microw. Theory Tech.* **34** 38–50

Canters R A M, Paulides M M, Franckena M, Mens J W and van Rhoon G C 2013 Benefit of replacing the sigma-60 by the sigma-eye applicator. A Monte Carlo-based uncertainty analysis *Strahlentherapie Onkol.* **189** 74–80

Cole K S and Cole R H 1941 Dispersion and absorption in dielectrics I. Alternating current characteristics *J. Chem. Phys.* **9** 341

de Greef M, Kok H P, Correia D, Borsboom P-P, Bel A and Crezee J 2011 Uncertainty in hyperthermia treatment planning: the need for robust system design *Phys. Med. Biol.* **56** 3233–50

Fenn A J 2008 *Adaptive Phased Array Thermotherapy for Cancer* 1st edn (Boston, MA: Artech House) p 70

Gabriel C 1996 Compilation of the dielectric properties of body tissues at RF and microwave frequencies *Brooks Air Force Tech Rep* AL/OE-TR:0037

Gabriel C, Gabriel S and Corthout E 1996a The dielectric properties of biological tissues: I. Literature survey *Phys. Med. Biol.* **41** 2231–49

Gabriel S, Lau R W and Gabriel C 1996b The dielectric properties of biological tissues: II. Measurements in the frequency range 10 Hz to 20 GHz *Phys. Med. Biol.* **41** 2251–69

Hafalir F S, Oran O F, Gurler N and Ider Y Z 2014 Convection-reaction equation based magnetic resonance electrical properties tomography (cr-MREPT) *IEEE Trans. Med. Imaging* **33** 777–93

Hahn G M *et al* 1980 Some heat transfer problems associated with heating by ultrasound, microwaves, or radio frequency *Ann. New York Acad. Sci.* **335** 327–51

Hasgall P *et al* 2015 IT'IS database for thermal and electromagnetic parameters of biological tissues Version 2.6 13 January 2015 (DOI: 10.13099/ViP-Database-V2.6)

Homann H 2012 SAR prediction and SAR management for parallel transmit MRI *PhD Dissertation*
Joines W T, Zhang Y and Li C J R 1994 The measured electrical properties of normal and malignant human tissues from 50 to 900 MHz *Med. Phys. Phys.* **21** 547–50
Katscher U, Abe H, Ivancevic M, Djamshidi K, Karkowski P and Newstead G 2013 Towards the investigation of breast tumor malignancy via electric conductivity measurement *Proc. 21st Annual Meeting ISMRM* (*Salt Lake City, USA*) p 3372
Katscher U, Voigt T, Findeklee C, Vernickel P, Nehrke K and Dössel O 2009 Determination of electric conductivity and local SAR via B1 mapping *IEEE Trans. Med. Imaging* **28** 1365–74
Kim M-O, Choi N, Shin J, Lee J and Kim D-H 2013 Phase unbanding in bSSFP for liver conductivity imaging at 3.0 T *Proc. 21st Annual Meeting ISMRM* (*Salt Lake City, USA*) p 4173
Kraszewski A, Stuchly M A, Stuchly S S and Smith A 1982 *In vivo* and *in vtiro* dielectric properties of animal tissues at radio frequencies *Bioelectromagnetics* **3** 421–32
Leussler C, Karkowski P and Katscher U 2012 Tempendent-dependent conductivity change using MR-based electric properties tomography *Proc. 20th Annual Meeting ISMRM* p 3451
Liu J, Zhang X, Schmitter S, Van de Moortele P-F and He B 2015 Gradient-based electrical properties tomography (gEPT): a robust method for mapping electrical properties of biological tissues *in vivo* using magnetic resonance imaging *Magn. Reson. Med.* **74** 634–46
Liu J, Zhang X, Van de Moortele P-F, Schmitter S and He B 2013 Determining electrical properties based on B1 fields measured in an MR scanner using a multi-channel transmit/receive coil: a general approach *Phys. Med. Biol.* **58** 4395–408
Marques J P, Sodickson D K, Ipek O, Collins C M and Gruetter R 2015 Single acquisition electrical property mapping based on relative coil sensitivities: a proof-of-concept demonstration *Magn. Reson. Med.* **74** 185–195
O'Rourke A P *et al* 2007 Dielectric properties of human normal, malignant and cirrhotic liver tissue: *in vivo* and *ex vivo* measurements from 0.5 to 20 GHz using a precision open-ended coaxial probe *Phys. Med. Biol.* **52** 4707–19
Osswald K 1937 Messung der Leitfahigkeit und Dielektrizitatkonstante biologischer Gewebe und Flussigkeiten bei kurzen Wellen *Hochfrequenz Tech Elektroakustik* **49** 40–50
Peyman A and Gabriel C 2012 Dielectric properties of porcine glands, gonads and body fluids *Phys. Med. Biol.* **57** N339–44
Peyman A, Gabriel C, Grant E H, Vermeeren G and Martens L 2009 Variation of the dielectric properties of tissues with age: the effect on the values of SAR in children when exposed to walkie-talkie devices *Phys. Med. Biol.* **54** 227–41
Peyman A, Rezazadeh A A and Gabriel C 2001 Changes in the dielectric properties of rat tissue as a function of age at microwave frequencies *Phys. Med. Biol.* **46** 1617–29
Peyman A, Rezazadeh A A and Gabriel C 2002 Corrigendum: changes in the dielectric properties of rat tissue as a function of age at microwave frequencies *Phys. Med. Biol.* **47** 2187–8
Rajewski B 1938 *Ultrakurzwellen, Ergebnisse der Biophysikalishen Forschung* Bd 1 (Leipzig: Georg Thieme)
Restivo M C *et al* 2016 Local specific absorption rate in brain tumors at 7 tesla *Magn. Reson. Med.* **75** 381–9
Saunders S R and Aragon Zavala A 2007 *Antennas and Propagation for Wireless Communication Systems* 2nd edn (New York: Wiley)
Schwan H P 1955 Application of uhf impedance measuring techniques in biophysics *IRE Trans. Med. Eletron.* **PGME-4** 75
Schmid G, Neubauer G and Illievich U M 2003 Dielectric properties of porcine brain tissue in the transition from life to death at frequencies from 800 to 1900 MHz *Bioelectromagnetics* **24** 413–22
Shin J *et al* 2014 Initial study on *in vivo* conductivity mapping of breast cancer using MRI *J. Magn. Reson. Imaging* **42** 371–8
Sodickson D K *et al* 2013 Generalized local maxwell tomography for mapping of electrical property gradients and tensors *Proc 21st Annual Meeting ISMRM* (*Salt Lake City, USA*) p 4175
Stehning C, Voigt T, Karkowski P and Katscher U 2012 Electric properties tomography (EPT) of the liver in a single breathhold using SSFP *Proc. 20th Annual Meeting ISMRM* (*Melbourne, VIC, Australia*) p 386
Stogryn A 1971 Equations for calculating the dielectric constant of saline water *IEEE Trans. Microw. Theory. Tech.* **19** 733–6
Stoy R D, Foster K R and Schwant H P 1982 Dielectric properties of mammalian tissues from 0.1 to l00 MHz: a summary of recent data *Phys. Med. Biol.* **27** 501–13

Stuchly M A, Athey T W, Stuchly S S, Samaras G M and Taylor G 1981 Dielectric properties of animal *in vivo* at frequencies 10 MHz–1GHz *Bioelectromagnetics* **2** 93–103

Surowiect A, Stuchlyt S S, Keaneys M and Swarup A 1986 *In vivo* and *in vitro* dielectric properties of feline tissues at low radiofrequencies *Phys. Med. Biol.* **31** 901–9

Trokhanova O V, Chijova Y A, Okhapkin M B, Korjenevsky A V and Tuykin S 2010 Using of electrical impedance tomography for diagnostics of the cervix uteri diseases *J. Phys. Conf. Ser.* **224** 012068

Van De Kamer J B, Van Wieringen N, De Leeuw A A C and Lagendijk J J W 2001 The significance of accurate dielectric tissue data for hyperthermia *Int. J. Hyperth.* **17** 123–42

Van Lier A L *et al* 2011 Electrical conductivity imaging of brain tumours *Proc. 19th Annual Meeting ISMRM* (*Montréal, QC, Canada*) p 4464

van Lier A L H M W 2012 Electromagnetic and thermal aspects of radiofrequency field propagation in ultra-high field MRI *PhD Dissertation*

van Lier A L H M W *et al* 2012a B1(+) phase mapping at 7 T and its application for *in vivo* electrical conductivity mapping *Magn. Reson. Med.* **67** 552–61

van Lier A L H M W *et al* 2013 Electrical properties tomography in the human brain at 1.5, 3, and 7T: a comparison study *Magn. Reson. Med.* **71** 354–63

van Lier A L H M W, van den Berg C A T and Katscher U 2012b Measuring electrical conductivity at low frequency using the eddy currents induced by the imaging gradients *Proc. 20th Annual Meeting ISMRM* (*Melbourne, VIC, Australia*) 3467

Voigt T, Homann H, Katscher U and Doessel O 2012 Patient-individual local SAR determination: *in vivo* measurements and numerical validation *Magn. Reson. Med.* **68** 1117–26

Voigt T, Katscher U and Doessel O 2011a Quantitative conductivity and permittivity imaging of the human brain using electric properties tomography *Magn. Reson. Med.* **66** 456–66

Voigt T, Väterlein O, Stehning C, Katscher U and Fiehler J 2011b *In vivo* glioma characterization using MR conductivity imaging *Proc. 19th Annual Meeting ISMRM* (*Montréal, QC, Canada*) p 2865

Yarnykh V L 2007 Actual flip-angle imaging in the pulsed steady state: a method for rapid three-dimensional mapping of the transmitted radiofrequency field *Magn. Reson. Med.* **57** 192–200

Yuan Y *et al* 2012 Utility of treatment planning for thermochemotherapy treatment of nonmuscle invasive bladder carcinoma *Med. Phys.* **39** 1170–81

Zhang X, Schmitter S, Van de Moortele P-F, Liu J and He B 2013 From complex B(1) mapping to local SAR estimation for human brain MR imaging using multi-channel transceiver coil at 7 T *IEEE Trans. Med. Imaging* **32** 1058–67